EJAR

Groundwater exploration at Rafah, Sinai Peninsula, Egypt

Mahmoud I. I. Mohamaden

National Institute of Oceanography and Fisheries, Alexandria, Egypt.
E-mail: Mahmoud_Moha12@Yahoo.com

Received 5th July 2009, Accepted 15th September 2009

Abstract

In order to investigate the Quaternary groundwater aquifers, 79 Vertical electrical soundings (V.E.S.'s) along 14 profiles were measured over the area of Rafah in northeast portion Sinai. The results of interpretation are used to construct the geoelectrical sections in light of the surface and subsurface geological information. Based on the resistivity results and depth of penetration are constructed to delineate the aquifer. The geoelectrical field investigates some knowledge of lithology and geological structural of the study area. In order to evaluate the Quaternary aquifer that may control the groundwater occurrence and quality of the subsurface layers in the Rafah area, northern Sinai.The inspection of litho-resistivity cross sections reveals the presence of three main geoelectrical layers. The first layer (a) is composed of gravels with relatively very high electrical resistivity values and thin thickness. Layer (b) is formed sand (main aquifer), and is characterized by relatively moderate electrical resistivity values (8-204 ohm-m) and depth range from 3.6 to 181 m. Layer (c) is formed from clay (aquiclude) with relatively low electrical resistivity values. Structurally, the area under investigation may be affected by two groups of faults. The central zone between these two groups of faults is probably bounding the groundwater and may include the fresh water. The thicknesses of this zone increase towards the southern direction. The down thrown side of these groups of faults divided into: the northern faults with down thrown side towards the southern direction. While the southern faults with down thrown side towards the northern direction. These faults are forming of graben.

Keywords: Groundwater, V.E.S., aquifer, Rafah.

1. Introduction

Pressure in natural resources from growing populations, with growing demands for water supply, infrastructure and housing, has increased in the past decade and can be expected to continue to rise. Further stress on the environment due to pollution will increase the need for detailed geological knowledge. The surface fresh water resources are relatively meager to cater the need of various nations. As such, groundwater resources are the most suitable resources to cover between the water demand and already available sources. Geophysical tools are the most suitable tools for searching to the groundwater.

The study area (Figure 1) is principally located the north eastern Sinai, between Latitude 30º 00` and 31º 19`N, and Longitude 33º 54` and 34º 15`E. this area is bounded by the Mediterranean Sea to the north and boundary between Egypt and Palestinian boarder the east.

Geologically, according to the results of drilled boreholes and the geological section performed by Diab (1998), the geological succession from top to bottom is discussed as follows:

1-Hollocene Deposits: It has variable thicknesses and consists mainly of:
a) Gravel, loam, sand calcareous in places, and silt in Wadi El-Arish.
b) Drift sand and loose essentially composed of loose Qz grains in the coastal and inland areas.
2- Pleistocene Deposits (80 m thick) it consists of:
a) Alluvial Deposits of Wadi El-Arish (10-50 m thick) composed of sand, calcareous silt and gravel.
b) Old beach deposits occurring within the coastal zone between El-Arish and west Rafah with variable thicknesses underlying dune sands, and mainly composed of sands, sandstone and clayey sands.
c) The Complex calcareous sandstone (Kurkur) which dominates the whole zone between the western vicinity of El-Arish town in the west Rafah in the east and southward to about 10 Km from the coastal line.

The Kurkur deposits are distinguished into two series:

- Upper Continental Kurkur, having a thickness of 20 m in few wells in Wadi El-Arish, to the north of the airport and east of El-Arish town. It occurs continues bed or inbeded in the alluvial deposits of Wadi El -Arish.
- Lower Marine Kurkur, having a thickness of about 40 m where it was penetrated in few wells in Wadi El-Arish

to the north of Lahfan. This series contain shell fragments. It is either overlain by the alluvial deposits in Wadi El-Arish or by old beach deposits in the coastal zone in the west of El-Arish town and underlined by the Pliocene facies.

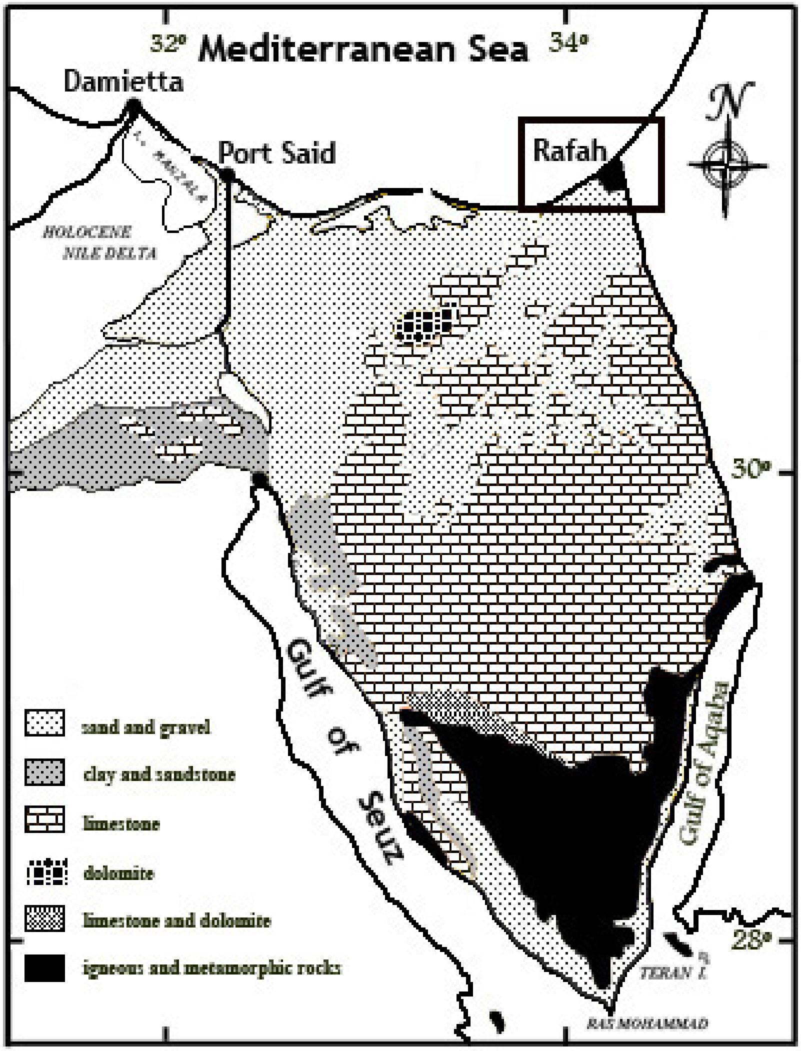

Figure 1: Area of study.

2. Geophysical data acquisition

In the present study geoelectrical resistivity field survey was carried out by applying the vertical electrical sounding (VES) technique which measures the electrical resistivity variation with depth. It is worth mentioning here that the electric resistivity of a rock formation varies according to the rock nature of material (density, porosity, pore size and shape), water content and its quality and temperature. Hence, there are no sharp limits for electric resistivity of porous formations. The resistivity is more controlled by the water contents and its quality within the matrix of the formation than by the solid granular resistivity value itself. Therefore, the geological unit may be subdivided into different geoelectrical units according to the different percentage of humidity within it. (Parasnis, 1997).

In present work, Schlumberger array was applied with half current electrode spacing (AB/2) starting from 1m to 1000 m. This spacing is sufficient to reach adequate depths covering the Quaternary aquifer in the study area (Abd El Fattah, 1994). A total number of 97 vertical electrical soundings were measured along 14 profiles (Figure 2). The sounding number 1 is located to the extreme south eastern part of the investigated area. These profiles run mainly from south to the north direction.

The geoelectrical resistivity measurements were performed applying two U.S.A. multimeter units of the type Fluke-27 allowing to filter the potential of the earth and measure the potential difference (ΔV) due to the fed current (I) and the current itself simultaneously. About 20% of the total measurements were recorded twice by changing the supply voltage. According to these repetitions the mean relative error for the field measurements was calculated and found to be ±1.45% or within the permissible limits.

The result of the geoelectrical survey was processed and quantitatively interpreted using available geological information and presented as geoelectrical sections along the various profiles. Many authors such as Koefoed (1965 b and c and 1960 a), Gosh (1971), Zohdy (1975 and 1989), and Hemeker (1984) studied the quantitative interpretation of the geoelectrical resistivity measurements. The interpretation of the apparent electrical resistivity data were achieved using two methods, the first is based on curve matching technique using Generalized Cagniard Graph method constructed by Koefoed (1960 a), in which the results obtained treated with the inverse problem method using computer programs constructed by Hemeker (1984).

2.1. Geoelectrical Sections

The data given in Table 1 is represented in form of section to highlight the nature of the different geoelectrical layers. Fourteen geoelectrical sections are constructed and discussed as follows:

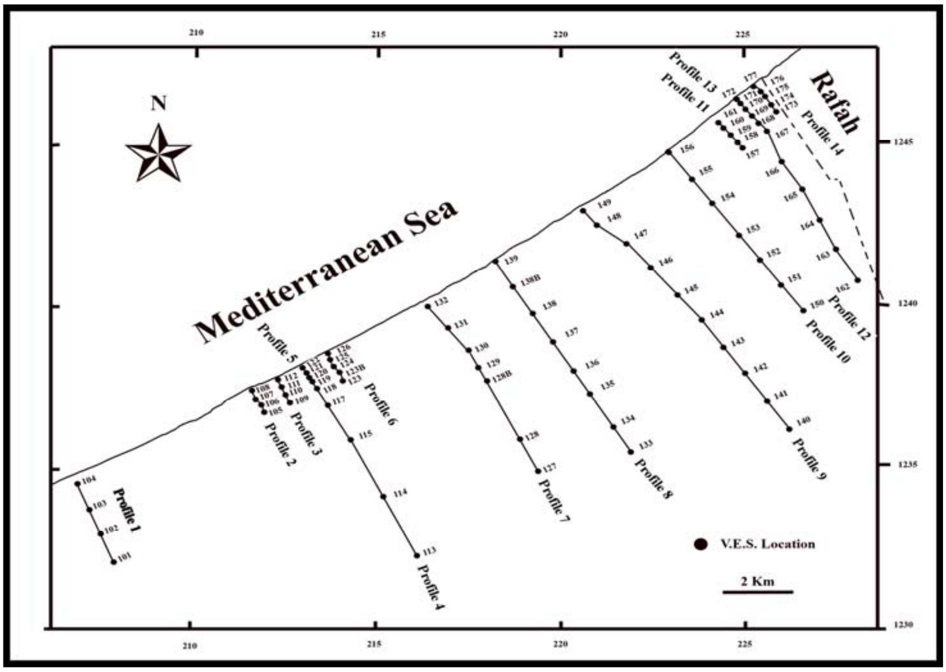

Figure 2: Location Map

Table 1: Geoelectrical Parameters of the Study Area.

V.E.S. no.	Layer 1		Layer 2		Layer 3		Layer 4		Layer 5
	ρ_1	d_1	ρ_2	d_2	ρ_3	d_3	ρ_4	d_4	ρ_5
101	**114**	1.1	**59**	6.3	**4**	123	**0.3**		
102	**38**	1.3	**58**	3.8	**3**	81.9	**0.3**		
103	**561**	1.2	**1020**	9.9	**62**	58	**2**		
104	**454**	0.31	**1070**	4.2	**254**	14.8	**8.5**	71.5	**2**
105	**353**	1.7	**4100**	6.4	**426**	12.8	**8**		
106	**196**	1.2	**413**	3	**73**	17	**18**	49.3	**1**
107	**487**	1.9	**61**	18.9	**5**	68.7	**0.4**		
108	**59**	0.73	**800**	1.8	**3**	27.3	**1**		
109	**1750**	1.7	**3210**	3.5	**1390**	15.6	**19.4**	80.2	**0.4**
110	**2440**	1.7	**120**	12	**14**	47.1	**2**		
111	**1000**	3.2	**253**	13.9	**14**	45.5	**1**		
112	**48**	0.79	**230**	1.9	**13**	14	**2**	97.4	**0.3**
113	**69**	1.3	**34**	1.7	**16**	25.1	**63**	63.1	**1**
114	**160**	1.8	**32**	14.3	**52**	21.4	**11**	80.7	**1**
115	**226**	2.2	**443**	4.6	**66**	11.3	**149**	60.2	**1**
117	**0.5**	0.91	**0.7**	7.9	**7**	52.2	**0.84**		
118	**1440**	1.2	**1250**	4.7	**632**	15.4	**73**	54.2	**4**
119	**2400**	0.95	**4610**	2.9	**2240**	13.4	**126**	50.7	**2**
122	**1330**	1.8	**392**	4.1	**6**	7.2	**4**	72	**0.4**
119	**2400**	0.95	**4610**	2.9	**2240**	13.4	**126**	50.7	**2**
120	**175**	0.98	**1490**	5.4	**61**	50.3	**1**		
121	**639**	1.3	**459**	6.7	**17**	24	**0.6**		
122	**1330**	1.8	**392**	4.1	**6**	7.2	**4**	72	**0.4**
123	**1430**	0.9	**1560**	14.4	**34**	57.4	**2.6**		
123B	**627**	1.2	**1770**	5.2	**190**	26.2	**18**	74.4	**1**
124	**74**	1.2	**940**	4.3	**10**	44.2	**1**		
125	**1200**	2.7	**351**	9.2	**8**	52.5	**1**		
126	**1620**	1.5	**159**	3.6	**5**	9.6	**1**	57.7	**0.3**
127	**324**	1.5	**136**	3.3	**26**	36.5	**1**		
128	**312**	1.5	**152**	17.2	**119**	43.9	**44**	132	**1**
128B	**86**	1.3	**145**	48.2	**1**				
129	**850**	1.5	**1160**	5	**62**	41.9	**2**		
130	**774**	0.78	**1260**	13.6	**68**	78	**2**		
131	**1980**	1.1	**3020**	1.9	**1020**	23.8	**28**	68.8	**5**
132	**3800**	2.2	**96**	8.1	**9**	52.9	**1**		
133	**419**	0.95	**179**	8.4	**52**	72.2	**0.82**		
134	**310**	1.3	**104**	9	**49**	181	**1**		
135	**319**	1.2	**143**	10.5	**80**	71.8	**39**	82.8	**4**
136	**247**	2	**107**	52.6	**4**				
137	**607**	1.1	**790**	6.1	**171**	50.9	**6**		
138	**757**	1.5	**1630**	3.9	**590**	10	**115**	60	**1**
138B	**2000**	0.44	**1600**	11.6	**121**	50.1	**6**		
139	**25**	1.2	**61**	4.1	**11**	30	**0.91**		
140	**193**	1.4	**126**	7.8	**12**	19.4	**69**	95.7	**4**
141	**188**	2	**8**	140	**2**				
142	**259**	1.8	**36**	26.1	**56**	109	**1**		
143	**156**	1	**38**	61.8	**3**				

Table 1: Continued

V.E.S. no.	**Layer 1**		**Layer 2**		**Layer 3**		**Layer 4**		**Layer 5**
	ρ_1	**d_1**	**ρ_2**	**d_2**	**ρ_3**	**ρ_1**	**d_1**	**ρ_2**	**d_2**
144	**335**	1	**275**	4.3	**41**	36	**9**		
145	**410**	1.8	**104**	55.1	**3**				
146	**1040**	0.8	**1170**	5.5	**416**	21.3	**24**	129	**0.4**
147	**1720**	0.9	**1840**	9.4	**24**	42	**7**		
148	**3720**	1.9	**2460**	7.3	**83**	43.2	**7**		
149	**2880**	1.1	**860**	5.9	**45**	37.4	**0.4**		
150	**126**	3.8	**32**	156	**6**				
151	**64**	0.79	**129**	115	**4**				
152	**109**	0.71	**112**	2.1	**57**	76.7	**7**		
153	**397**	0.82	**860**	12.9	**74**	83.2	**6**		
154	**633**	0.94	**1400**	16.7	**210**	47.5	**2**		
155	**1120**	0.94	**2770**	3.3	**1020**	16	**99**	85.2	**7**
156	**352**	1.2	**910**	3.3	**28**	57.3	**2**		
157	**890**	1.9	**820**	14.1	**47**	58	**8**		
158	**1000**	1	**1960**	13.4	**100**	72.3	**8**		
159	**2310**	2.4	**551**	17.1	**90**	67.6	**5**		
160	**632**	4.9	**46**	54.7	**2**				
161	**870**	0.72	**5950**	2.9	**51**	42.9	**3**		
162	**114**	1.5	**78**	6.2	**29**				
163	**28**	0.7	**204**	2.5	**18**	8.4	**77**	117	**23**
164	**152**	2.7	**303**	6.8	**77**				
165	**219**	0.62	**3220**	1.9	**215**	15	**30**		
166	**234**	0.73	**2290**	3.3	**217**	24.8	**11**		
167	**1110**	0.95	**1390**	22.7	**74**	118	**9.6**		
169	**2320**	43.5	**100**	104	**23**	124.6	**4**		
172	**340**	3.2	**10**	13	**30**	60.7	**1**		
168	**1380**	23.1	**460**	62	**30**	146.5	**5**		
169	**2320**	43.5	**100**	104	**23**	124.6	**4**		
170	**4270**	5.3	**840**	16	**30**	30.4	**90**	104	**6**
171	**490**	7.3	**20**	16.2	**50**	77.3	**2**		
172	**340**	3.2	**10**	13	**30**	60.7	**1**		
173	**2350**	0.83	**2500**	13.3	**84**	63.5	**9**		
174	**757**	1	**2800**	2.4	**990**	9.7	**32**	90.1	**0.3**
175	**60**	0.9	**32**	5.3	**44**	64.2	**0.7**		
176	**72**	2.7	**37**	57	**2**				
177	**20**	10.8	**43**	36.4	**3**				

Note: ρ= True resistivity (ohm-m) d = depth (m)

Profile 1

This profile is composed of 4 V.E.S.'s (101, 102, 103 and 104) and is located at the extreme south western portion of the study area. The three geoelectrical layers are described as follows (Figure 3 and Table 1):

a- Gravel

This layer is covered the area north of V.E.S. 102 with relatively highly electrical resistivity values (454–1070 ohm–m) and thicknesses (4.2–9.9 m).

b- Sand

This layer covered the ground surface of the area south of V.E.S. 103, which lies above the sea level, with relatively moderate electrical resistivity values (38–114 ohm–m). It is considered as the main aquifer. The thicknesses of this layer ranges from 3.8 to 6.3 m. While the area north of V.E.S. 102, this layer is covered by the gravel layer. It is characterized by relatively moderate electrical resistivity values (62–254 ohm–m) with thicknesses ranges from 14.8 to 58 m. This layer mainly under the sea level, then, it may be contaminated with gravel and salt water intrusion.

c- Clay

At the maximum depth of penetration along this profile, a clay layer with relatively low electrical resistivity values (0.3–8.5 ohm–m) is detected.

Structure

At the area between V.E.S.'s 102 and 103, we can detect a fault with down thrown side towards the north direction which barrier the seepage of the saltwater intrusion to the southern part of this profile.

Profile 2

It is composed of V.E.S.'s 105, 106, 107 and 108. Figure 4 and Table 1 show the geoelectrical section represents this profile:

a- Gravel

The upper most layer is represented by gravel which is characterized by relatively high electrical resistivity values (413–4100 ohm–m) and thin thicknesses (1.8–6.4 m).

b- Sand

This layer is detected only at the area south of V.E.S. 108 to the area north of V.E.S. 105. It is characterized by relatively moderate electric resistivity values (61–73 ohm–m) and depth from 17 to 68.7 m. It represents the main aquifer at this area. This layer seems to have a lenticular shape.

c- Clay

This layer is continuous and is in direct contact with the superficial layer at V.E.S.'s 105 and 108. It is characterized by relatively low electrical resistivity values (0.4–18 ohm–m).

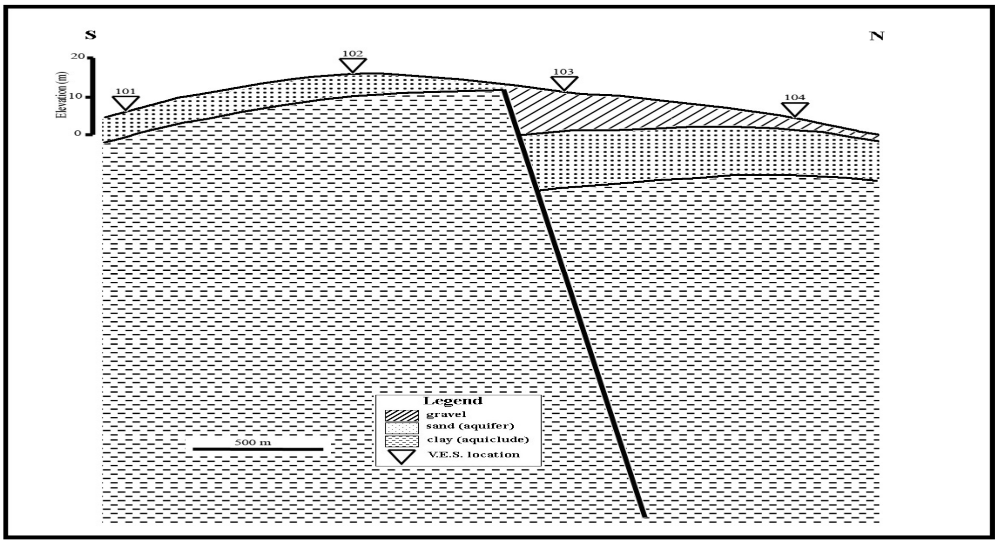

Figure 3: Geoelectrical Section of Profile 1

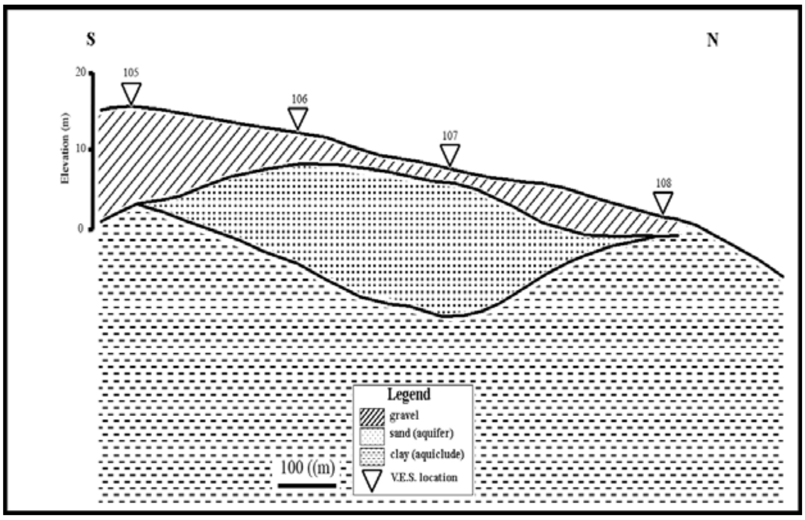

Figure 4: Geoelectrical Section of Profile 2

Profile 3

It is composed of V.E.S.'s 109, 110, 111 and 112. The geoelectrical section is shown by Figure 5 and Table 1:

a- Gravel

This layer covered all the ground surface of this profile. It is characterized by relatively high electric resistivity values (1000–3210 ohm–m). Sometimes, the resistivity values ranges from 120 to 253 ohm–m according to the salt water intrusion or the percentage of sand. This layer reached it's thicknesses from 1.9 to 15.6 m.

b- Sand

This layer characterized by relatively moderate electric resistivity values (13–19 ohm–m) and variable depth (14–80.2 m) increase towards the southern direction. It is considered as a main aquifer.

c- Clay

It is detected at the maximum depth of penetration and is characterized by relatively low electrical resistivity values (0.3–2 ohm–m). It considered as an aquiclude.

Structure

This profile is affected most probably by a fault south of V.E.S. 112 with down thrown side towards the southern direction.

Profile 4

It is composed of by V.E.S.'s 113, 114, 115, 117, 118, 119 and 122. The geoelectrical section is shown by Figure 6 and Table 1:

a- Gravel

This layer is mainly deposited at the northern part of V.S.E. 117 with relatively high electrical resistivity values (392–4610 ohm–m) and thin thicknesses increasing towards the southern direction (9.1-15.4 m). Also, this layer is detected under V.E.S.'s 114 and 115 with electrical resistivity values from 160 to 443 ohm–m according to percentage of sand content. Its thicknesses range from 1.8 to 4.6 m.

b- Sand

This layer is recorded along all over this profile with exception under V.E.S. 122 (main aquifer). It is characterized by relatively moderate electric resistivity values (11–126 ohm–m) with depth increase towards the southern direction (50.7–80.7 m).

c- Clay

It is recorded at the maximum depth of penetration with relatively low electrical resistivity values (0.8–6 ohm–m). This layer located beneath the sand layer all over this profile with exception of V.E.S. 122, Where it is deposited directly under the gravel layer.

Structure

This profile is affected probably by two faults at V.E.S. 117 and south of V.E.S. 122 with down thrown side towards the central part of this profile.

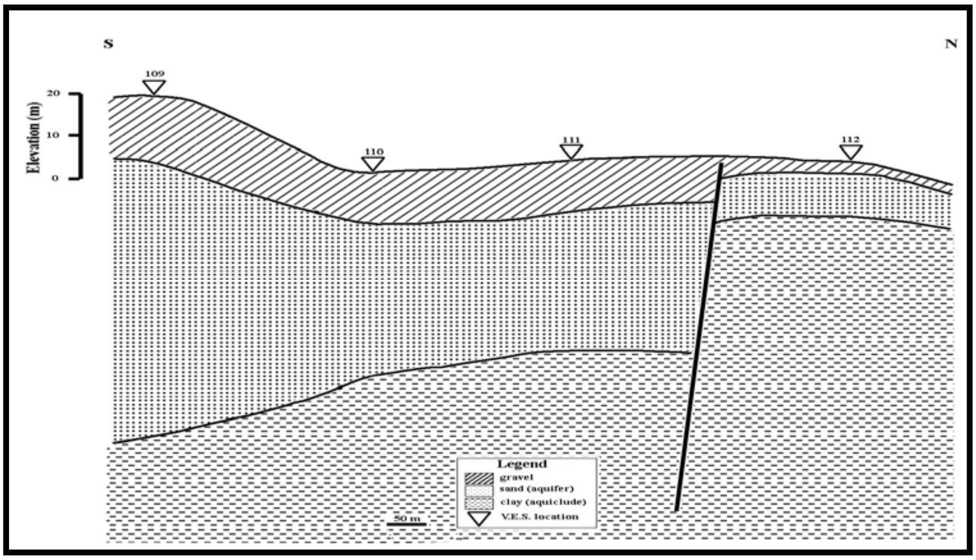

Figure 5: Geoelectrical Section of Profile 3

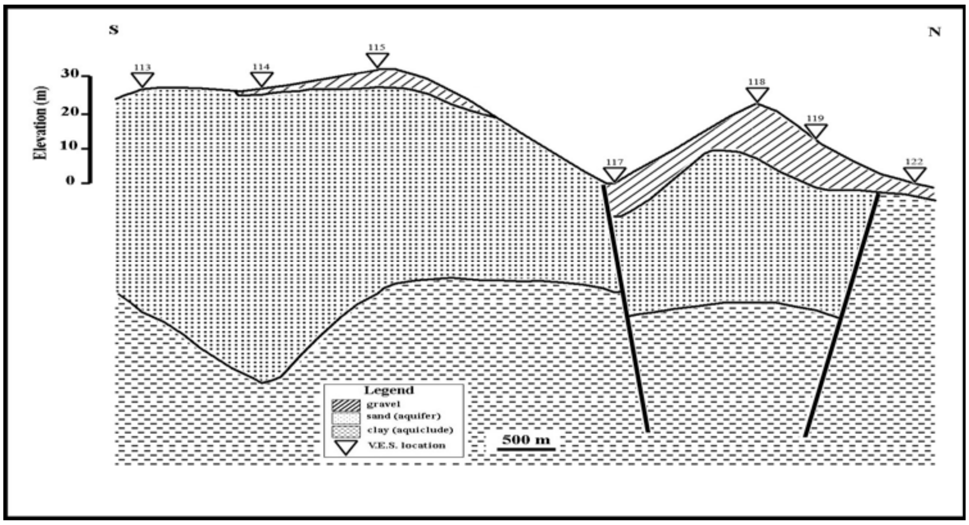

Figure 6: Geoelectrical Section of Profile 4

Profile 5

This profile is composed of 4 V.E.S.'s (119, 120, 121 and 122). The geoelectrical section is shown by Figure 7 and Table 1:

a- Gravel

This layer covered the ground surface of this profile with relative high electrical resistivity values (392-4610 ohm–m) and thin thicknesses (4.1–13.4 m). The thickness of this layer increases their thicknesses towards the southern direction.

b- Sand

This layer lies below the sea level, with relatively moderate electrical resistivity values ranging from 17 to 126 ohm–m. The resistivity values decrease towards the northern direction due to the seepage of the salt water. It is considered as the main aquifer. The thicknesses of this layer ranges from 24 to 50.7 m. Its thicknesses decrease towards the northern direction with disappearance north of V.E.S. 122.

c- Clay

At the maximum depth of penetration along this profile, a clay layer with relatively low electrical resistivity values (0.4–2.4 ohm–m) is detected. It is considered as aquiclude.

Structure

At the area between V.E.S.'s 121 and 122, a fault with down thrown side towards the southern direction. It is considered as barrier the seepage of the saltwater intrusion to the southern part of this profile.

Profile 6

It is composed of V.E.S.'s 123, 123B, 124, 125 and 126. The geoelectrical section is shown by Fig. 8 and Table 1:

a- Gravel

This layer covered all the ground surface of this profile. It is characterized by relatively very high electric resistivity values (351-1770 ohm–m). This layer reached it's thicknesses from 1.5 to 14.4 m. The general trend of increase of the thicknesses of this layer is from the north to the southern direction.

b- Sand

This layer characterized by relatively moderate electric resistivity values (8–190 ohm–m) and variable depth (3.6–74.4 m). It is considered as a main aquifer.

c- Clay

It can be detected at the maximum depth of penetration. It is characterized by relatively low electrical resistivity values (0.3–3 ohm–m). It considered as an aquiclude.

Structure

This profile is affected by a well detected fault south of V.E.S. 126 with down thrown side towards the southern direction. This fault reduces the thicknesses of the sand layer around of V.E.S. 126.

Profile 7

It is composed of V.E.S.'s 127, 128, 128B, 129, 130, 131 and 132. The geoelectrical section concluded that (Fig. 9& Table 1):

a- Gravel

This layer mainly deposited at the northern part of V.S.E. 128B with relatively high electrical resistivity values (312–3800 ohm–m) and thin thicknesses increase towards the northern direction (1.5-23.8 m).

b- Sand

This layer can be recorded along all over this profile (main aquifer). It is characterized by relatively moderate electric resistivity values (28–152 ohm–m) with depth mainly increase towards the central part of this profile (8.1–132 m).

c- Clay

It can be recorded at the maximum depth of penetration with relatively low electrical resistivity values (0.82–6 ohm–m). This layer located beneath the sand layer all over this profile.

Structure

This profile is affected by two pronounced faults south V.E.S. 128 and south of V.E.S. 132 with down thrown side towards the central part of this profile.

Profile 8

It is composed of V.E.S.'s 133, 134, 135, 136, 137, 138, 138B and 139. The geoelectrical section concluded that (Fig. 10& Table 1):

a- Gravel

This layer covered the ground surface of this profile with exception at V.E.S. 139. It characterized by relatively high electrical resistivity values (247-2000 ohm-m) and thin thicknesses (0.44-11.6 m). This layer mainly lies above the sea level.

b- Sand

It considered the main aquifer at the area under investigation. It can be detected under the gravel layer all over this profile with exception at V.E.S. 139. At V.E.S. 139 it covered the ground surface. It characterized by relatively moderate electrical resistivity values (11-179 ohm-m) and variable depth (4.1-181 m). The maximum depth of this layer may be located at the central part of this profile.

c- Clay

It can be recorded at the maximum depth of penetration with relatively low electrical resistivity values (0.82–6 ohm–m). This layer located beneath the sand layer all over this profile.

Structure

This profile affected by two faults north V.E.S. 133 and south of V.E.S. 139 with down thrown side towards the central part of this profile

.

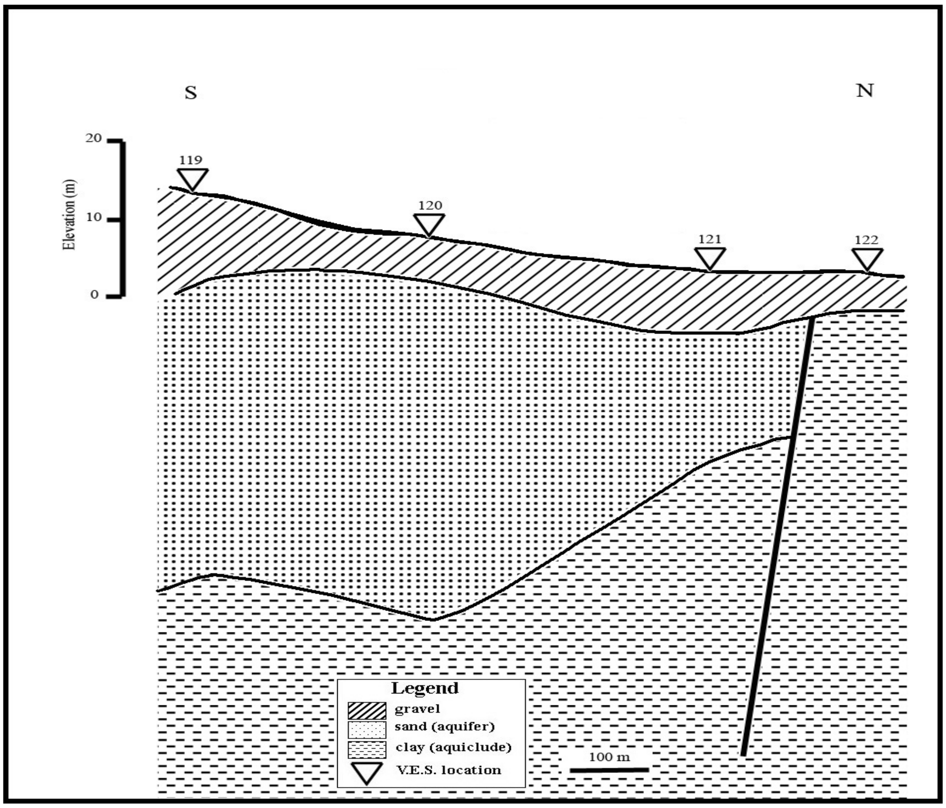

Figure 7: Geoelectrical Section of Profile 5

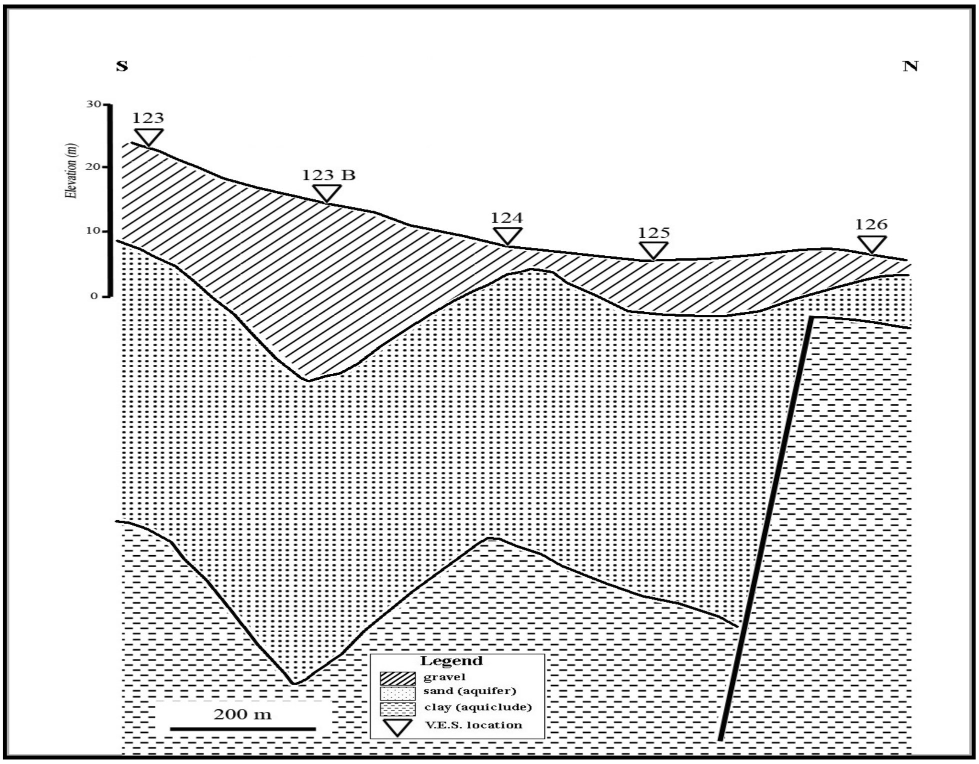

Figure 8: Geoelectrical Section of Profile 6

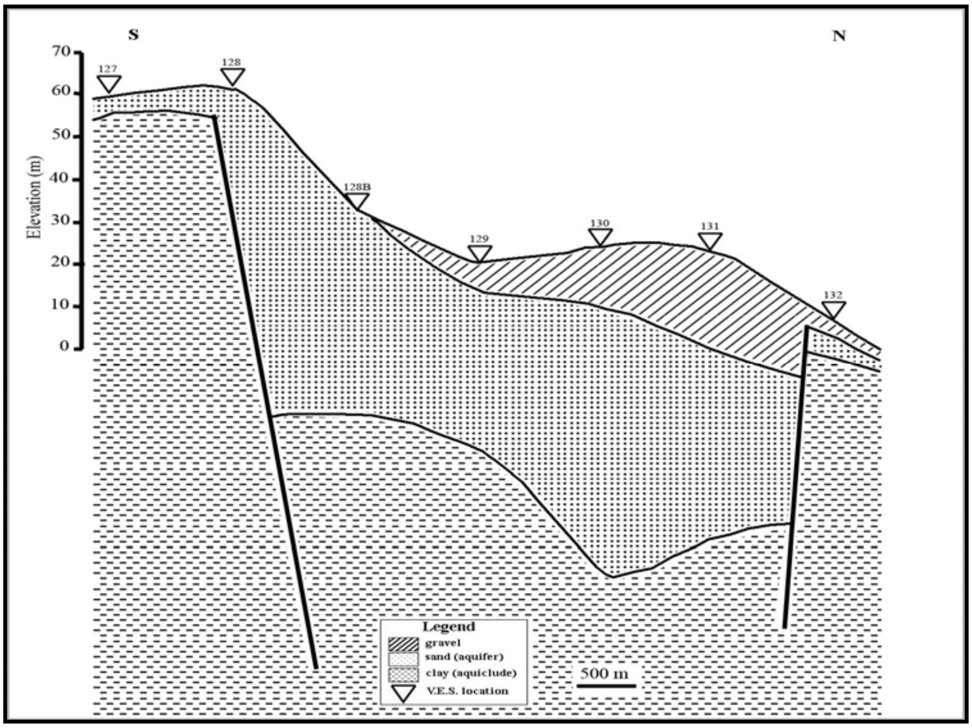

Figure 9: Geoelectrical Section of Profile 7

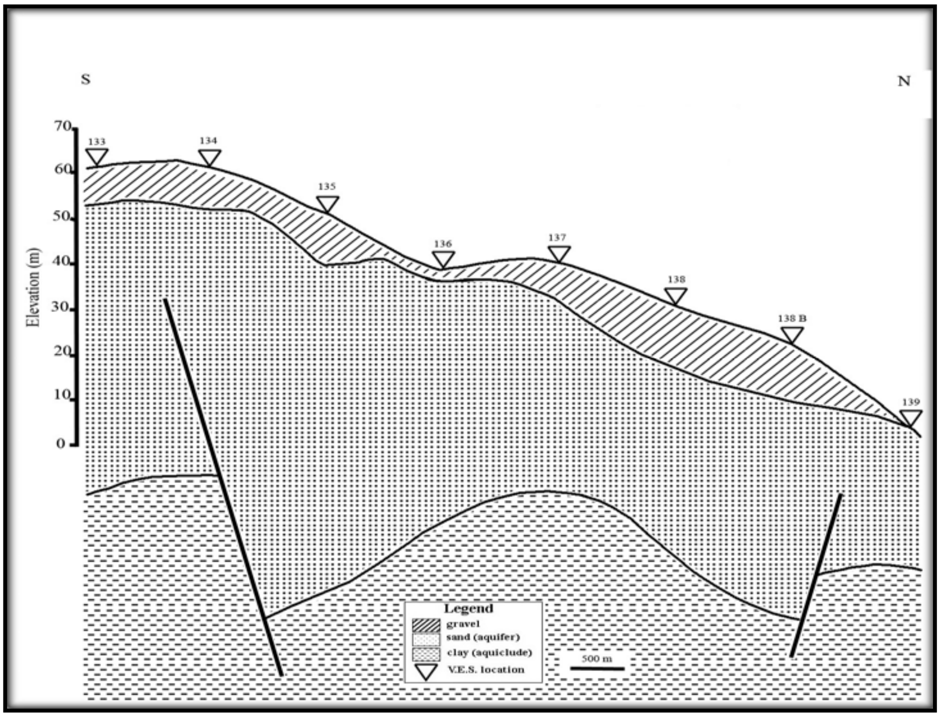

Figure 10: Geoelectrical Section of Profile 8

Profile 9

It is composed of V.E.S.'s 140, 141, 142, 143, 144, 145, 146, 147, 148 and 149. The geoelectrical section concluded (Fig. 11& Table 1):

a- Gravel

This layer mainly deposited at the ground surface all over this profile. It characterized by relatively high electrical resistivity values (126–3720 ohm–m) and thin thicknesses (1-21.3 m). At the northern part of this profile, this layer characterized by relatively high electrical resistivity values due to the dryness of lithology. While, the southern part is less in electrical resistivity values.

b- Sand

This layer can be recorded along all over this profile is considered as a main aquifer. It is characterized by relatively moderate electric resistivity values (12–104 ohm–m) with depth mainly increase towards the central part of this profile (36–129 m).

c- Clay

It can be recorded at the maximum depth of penetration with relatively low electrical resistivity values (0.4–9 ohm–m). This layer located beneath the sand layer all over this profile (aquiclude).

Structure

This profile affected by the same figure two faults of profile 7 & 8 at V.E.S. 141 and at V.E.S. 147 with down thrown side towards the central part of this profile.

Profile 10

It is composed of V.E.S.'s 150, 151, 152, 153, 154, 155 and 156. The geoelectrical section concluded that (Fig. 12&Table 1):

a- Gravel

This layer can be detected the area north of V.E.S. 152. It characterized by relatively high electrical resistivity values (352-2770 ohm-m) and thicknesses range from 3.3-16.7 m.

b- Sand

It is a main aquifer of the area under investigation. It characterized by relatively moderate electrical resistivity values (32-126 ohm-m). It lies mainly above the sea level. It's depth range from 47.5 to 156 m. The maximum thicknesses located at the central part of this profile.

c- Clay

It considered as aquiclude. It characterized by relatively low electrical resistivity values (2-6 ohm-m).

Structure

This profile is still affected by the same figure two faults located at the northern part of V.E.S. 150 and south of V.E.S. 155 with down thrown side towards the central part of this profile.

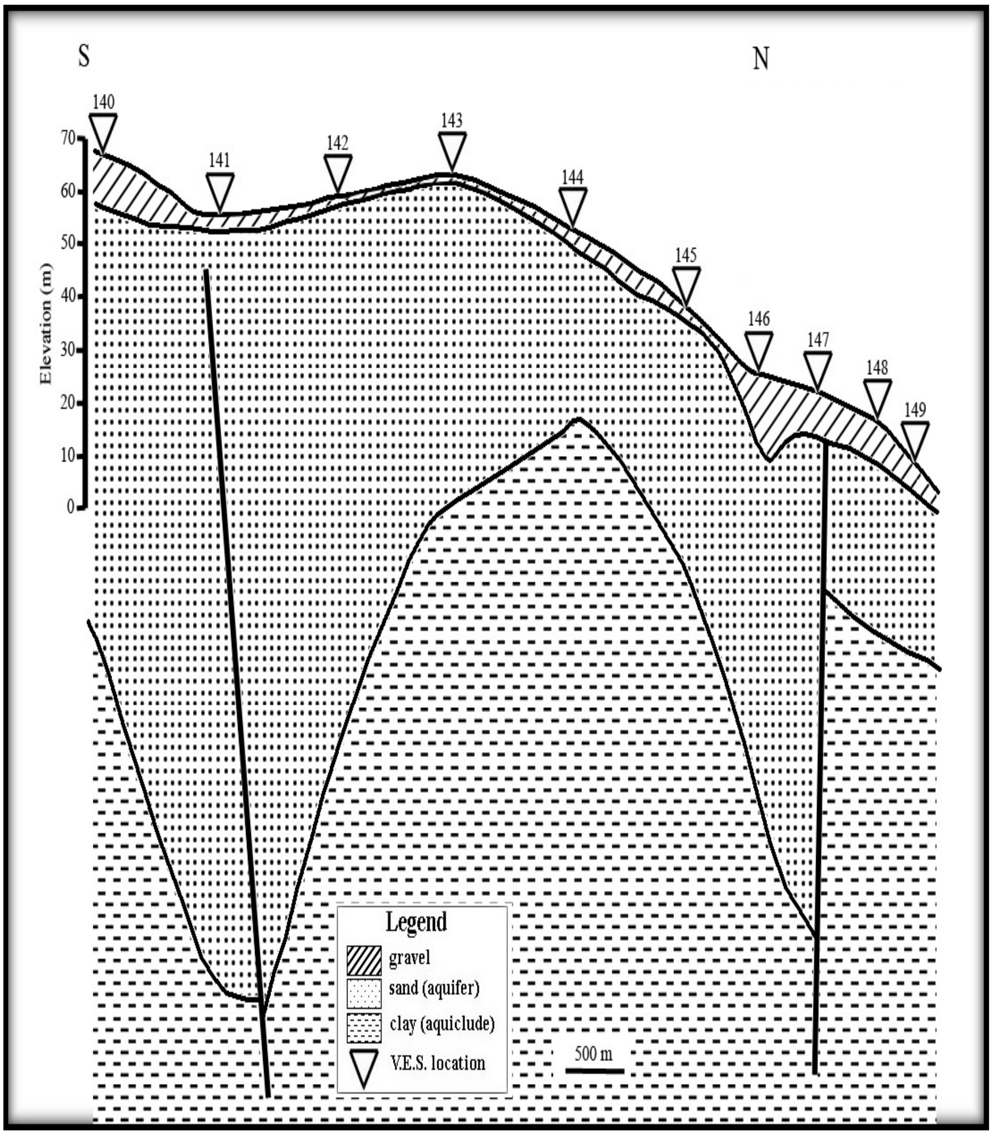

Figure 11: Geoelectrical Section of Profile 9

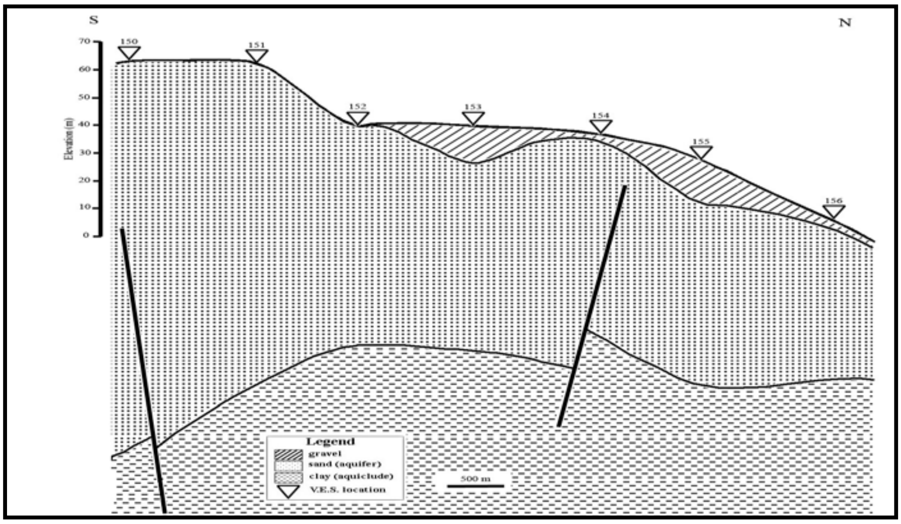

Figure 12: Geoelectrical Section of Profile 10

Profile 11

This profile is composed of 5 V.E.S.'s (157, 158, 159, 160 and 161). The geoelectrical section shows that (Fig. 13& Table 1):

a- Gravel

This layer covered the ground surface of this profile mainly increase their thicknesses towards the southern direction (2.9-17.1 m). It characterized by relatively high electrical resistivity values (551-5950 ohm-m).

b- Sand

It is the main aquifer at this area. It characterized by relatively moderate electrical resistivity values (47-100 ohm-m). Its depth range from 42.9-72.3 m. The thicknesses of this layer increase towards the central part of this profile.

b- Clay

It located at the maximum depth of penetration along this profile. It characterized by relatively low electrical resistivity values (2-8 ohm-m)

Profile 12

This profile is composed of 8 V.E.S.'s (162, 163, 164, 165, 166, 167,169 and 172). The geoelectrical section deduced that (Fig. 14& Table 1):

a- Gravel

This layer mainly deposited at the ground surface of this profile with relatively high electrical resistivity values (114–2320 ohm–m) and thin thicknesses increase towards the central part of this profile. The depth of this layer range from 1.5 to 43.5 m.

b- Sand

This layer can be recorded along all over this profile (main aquifer). It is characterized by relatively moderate electric resistivity values (10–78 ohm–m) with depth reached to the maximum depth of penetration as the area south of V.E.S. 167 or till depth from 60.7 to 124.6 m at the maximum northern part of this profile.

c- Clay

It can be recorded at the maximum depth of penetration at the area north of V.E.S. 167 with relatively low electrical resistivity values (1–4 ohm–m).

Structure

This profile is affected by the two faults (near the end of the stripped area) around of V.E.S. 162 and around of V.E.S. 167 with down thrown side towards the central part of this profile.

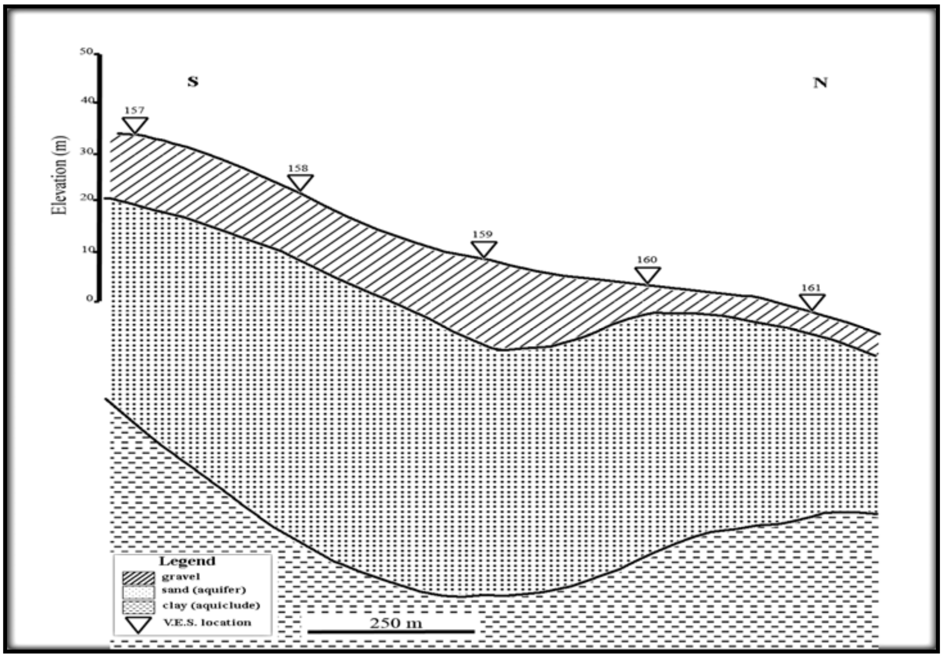

Figure 13: Geoelectrical Section of Profile 11

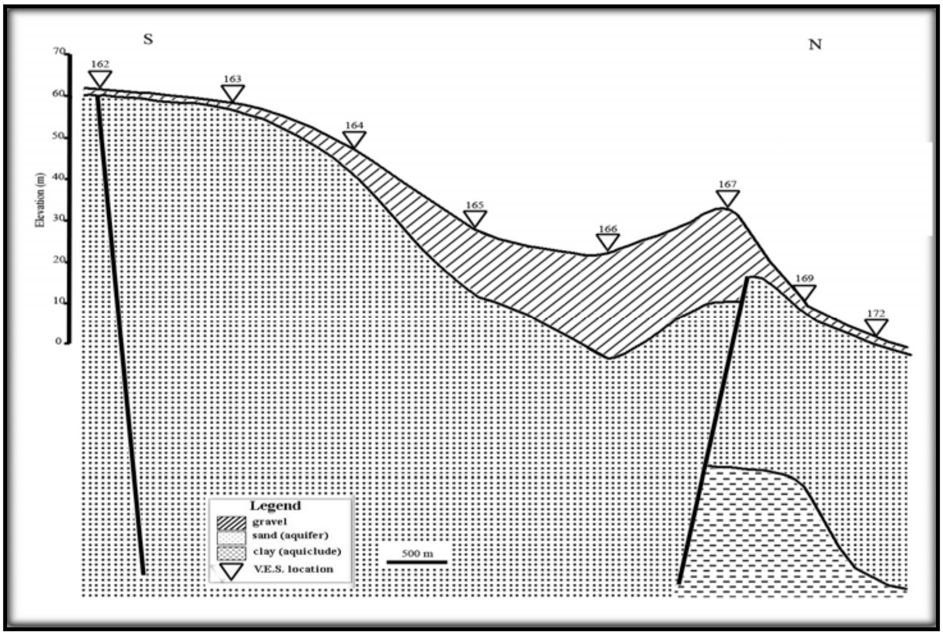

Figure 14: Geoelectrical Section of Profile 12

Profile 13

This profile is composed of 5 V.E.S.'s (168, 169, 170, 171 and 172). The geoelectrical section deduced that (Fig. 15& Table 1):

a- Gravel

This layer covered the ground surface of this profile. It characterized by relatively very high electrical resistivity values (340–4270 ohm–m) and thin thicknesses (3.2-62 m). The thicknesses of this layer decrease towards the northern direction

b- Sand

This layer can be detected under the gravel layer along this profile. It is characterized by relatively moderate electric resistivity values (10-100 ohm–m) and depth from 60.7 to 146.5 m. It considered the aquifer at this area. The thicknesses of this layer decrease towards the northern direction

c- Clay

At the maximum depth of penetration, this layer can be detected. It is characterized by relatively low. electrical resistivity values (1–6 ohm–m). This layer considered as aquiclude.

Profile 14

It is composed of V.E.S.'s 173, 174, 175, 176 and 177. The geoelectrical section shows that (Fig. 16& Table 1):

a- Gravel

This layer covered the ground surface of the area south of V.E.S. 175. It characterized by relatively very high electrical resistivity values (990–2800 ohm–m) and thin thicknesses (9.7–13.3 m).

b- Sand

This layer can be detected at the ground surface at the area north of V.E.S. 175 or under the gravel layer at the area south of V.E.S. 175. It is characterized by relatively moderate electric resistivity values (20–84 ohm–m) and depth from 36.4 to 90.1 m. It considered the aquifer at this area.

c- Clay

At the maximum depth of penetration, this layer can be detected. It is characterized by relatively low electrical resistivity values (0.3–9 ohm–m). This layer considered as aquiclude

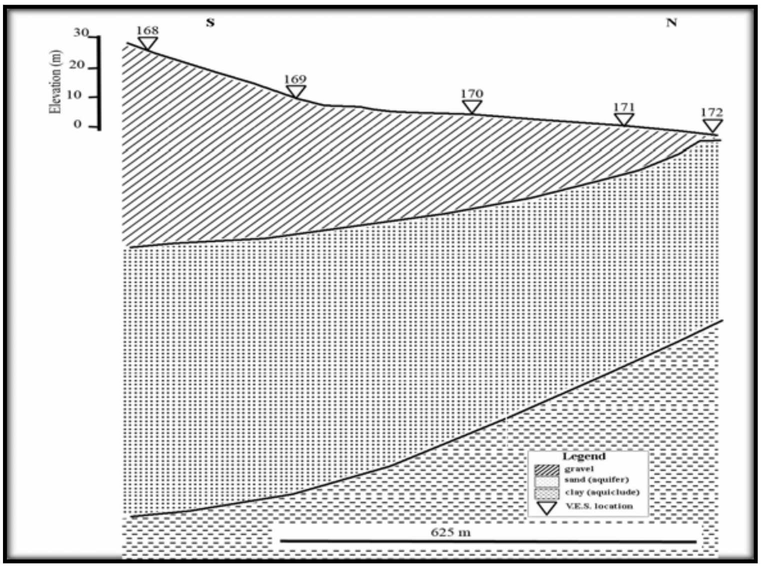

Figure 15: Geoelectrical Section of Profile 13

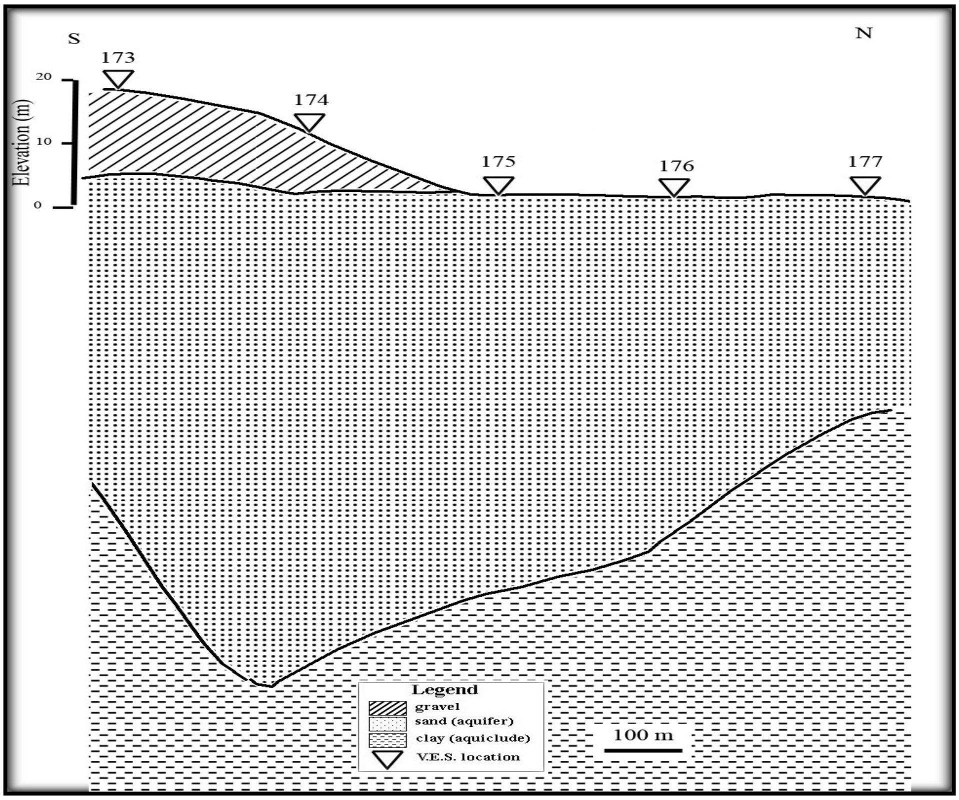

Figure 16: Geoelectrical Section of Profile 14

3. Result and Conclusions

The subsurface layers in the area under investigation are divided into three geoelectrical layer as follows:

The superficial geoelectrical layer is characterized by relatively high electrical resistivity values (340-5950 ohm-m). It is formed of gravel sometimes intercalated with sand and clay (sabkha). Sabkha is characterized by relatively low electric resistivity values (120-253 ohm-m). The thicknesses of this layer ranges from 1 to 43.5 m. It is covered the ground surface. Sometimes, it can not detect.

The second geoelectrical layer is formed of sand (aquifer). It is characterized by relatively moderate electrical resistivity values (8-204 ohm-m) and variable depth (3.6-181 ohm-m). Mostly, this layer is covered by the gravel layer and rarely covered the ground surface. Sometimes, this layer can be extended to the maximum depth of penetration.

The third geoelectrical layer formed of clay (aquiclude). It is characterized by relatively low electrical resistivity values (0.3-18 ohm-m). It is extends to the maximum depth of penetration.

Structurally, the area under investigation is affected by two groups of faults. The down thrown side of these faults divided into: the northern faults with down thrown side towards the southern direction. While the southern faults with down thrown side towards the northern direction. These faults are forming a graben.

The central zone is most probably bounding the groundwater and may include the fresh water (Fig.17). The thicknesses of this zone increase towards the southern direction.

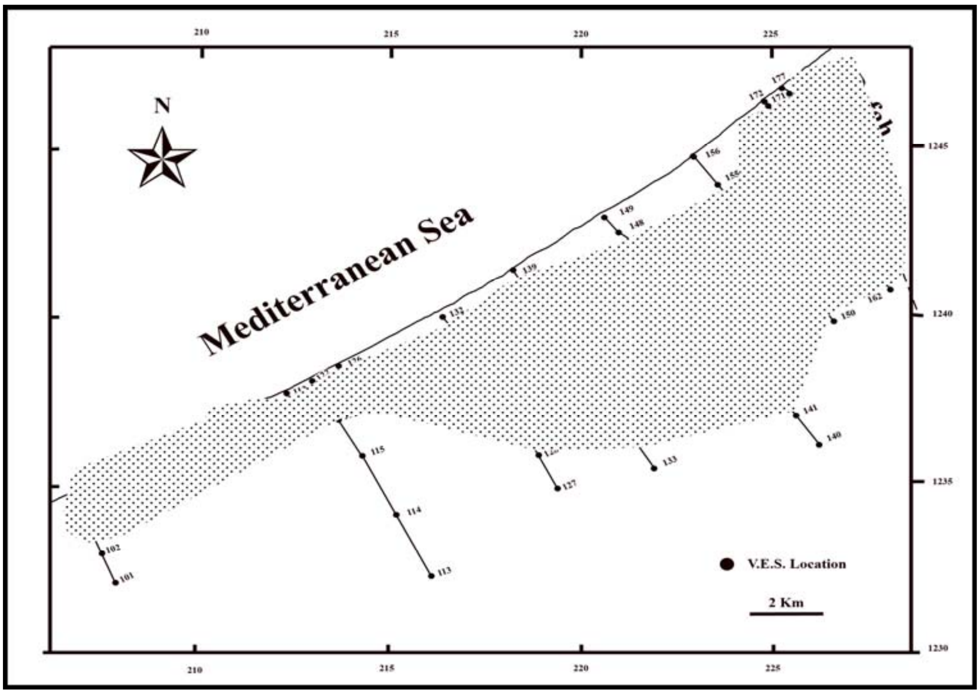

Figure 17: Structural Affecting the Area under Investigation

References

Abd Alla, M.A., El-Qady, G., and Fathy, R.: 2005, Groundwater exploration using geophysics at wadi EL-Assuity, Eastern Desert, Egypt. *Journal of Geophysics,* 4(1): 23-34.

Abd El Fattah, Th.: 1994, Current Penetration and Depth Investigation in Schlumberger Configuration. *Buletin of Faculty of Science, Qena Univ. Egypt*, 41-48.

Abd El-Rahman, A., and Khaled, M.A.: 2005, Geophysical Exploration for Groundwater Possibilities in Wadi El-Rahba, Eastern Desert. Egypt. *Geophysical Society Journal,* 3(1): 99-108.

Al-Abaseiry, A., Abdel Rahman and Ezz El-Deen, M.M.: 2005, Geophysical Exploration for Groundwater Potientialities in Wadi El-Rahba, Eastern Desert, Egypt. *Geophysical Society Journal*, 3(1): 119-1128.

Alotaibi, A.M. and AlAmri, A.M.: 2007, Ground Water Potentialities of Wadi Malakan-Southern Makkah AlMokadash City, Saudi Arabia. *Geophysical Society Journal*, 5(1): 101-116.

Barker, R.D.: 1980, Application of geophysics in groundwater investigations. *Water Survery,* 84: 489-492.

Bernard, J. and Valla, P.: 1991, Groundwater exploration in fissured media with electric and VLF methods. *Geoexploration,* 27: pp. 81-91.

Diab, A. F.: 1998, Geology, pedology and hydrology of the Quaternary deposits in Sahl El Tinah area and its vicinities for future development of north Sinai, Egypt. Ph. D. Thesis. Faculty of Science, Mansoura University, Egypt, 242p.

El Alfy M. and Merkel, B.: 2006, Hydrochemical relarionships and geochemical modeling of ground water in al arish area, nort Sinai, Egypt. *Hydrological Science and Technology*, 22(1-4): 47-62.

Gaber, S., El-Fiky, A.A., Abou Shagar, S. And Mohamaden, M.: 1999, Electrical Resistivity Exploration of the Royal Ptolemic Necropolis in the Royal Quarter of Ancient Alexandria, Egypt. *Archaeological Prospection,* 6: 1-10.

Gosh, D.A.: 1971, The application of geoelectrical resistivity measurements. *Geophysical Prospecting,* 19: 192-217.

Hemeker, C.J.: 1984, Vertical electrical sounding model interpretation program, IWCO, The Netherlands.

Hosny, M.M., EZZ El-Deen, Abdallah, A.A., Abdel Rahman and Barseim, M.S.M.: 2005, Geoelectrical Study on the Groundwater Occurrence in the Area Southwest of Sidi Barrani, Northwestern Coast, Egypt. *Geophysical Society Journal,* 3(1): 109-118.

Ibrahim, E.H., Shereef, M.R., El Galladi, A.A.and Pederson, L.B.: 2004, Geoelectric Study on Quaternary Groundwater Aquifers in Northwest

Sainai, Egypt. *Geophysical Society Journal*, 2(1): 69-74.

Koefoed, O.: 1960 a, A generalized Cagniard graph for the interpretation of geoelectrical sounding data. *Geophysical Prospecting*, 8: 459-469.

Koefoed, O.: 1965 b, A semi direct method of interpreting resistivity observations. *Geophysical Prospecting,* 13(2): 259-282.

Koefoed, O.: 1965 c, A direct methods of interpreting resistivity observations. *Geophysical Prospecting,* 13(4): 568-591.

Mesbah, M.A.: 2003, Groundwater Environmental Prospection Using Electrical Resistivity Survey at the New Kattamiya City, Near Cairo, Egypt. *Annals of Geological Survey of Egypt*, XXVI: 409-420.

Mohamaden, M.I.I.: 2005, Electric Resistivity Investigation at Nuweiba Harbour of Aqaba, South Sinai, Egypt. *Egyptian Journal of Aquatic Research,*31(1): 58-68.

Mousa, D.A.: 2003, The role of 1-D sounding and 2-D resistivity inversions in delineating the near-surface lithologic variations in Tushka area, south of Egypt. *Geophysical Society Journal*, 1: 57-64.

Nigm, A.A., elterb, R. A., Nasr, F.E. and Thobaity, H. M.: 2008, Contribution of Ground Magnetic and Resistivity Methods in Groundwater Assessment in Wadi Bany Omair. Holy Makkah Area, Saudi Arabia, Egyptian. *Geophysical Society Journal,* 6(1): 67-79.

Nowroozi, A.; Horrocks, B. and Henderson, P.: 1999, Saltwater intrusion into the freshwater aquifer in the eastern shore of Virginia: a reconnaissance electrical resistivity survey. *Journal of Applied Geophysics*, 42: 1-22.

Parasnis, D.: 1997, Principle of Applied Geophysics, London: Chapman and Hall., 275p.

RIGW/IWACO B.V., EMGR.: 1997, Water Quality Monitoring Programme, (TN/70.00067/WQM/97/20).

Said, R.: 1981, The geological evaluation of the River Nile, *Springer-verlag, New York,* 174p.

Van Overmeeren, R.: 1989, Aquifer boundaries explored by geoelectrical measurements in the coastal plain of Yemen, A case of equivalence. *Geophysics,* 54: 38-48.

Youssef, A.M.A., Abdellatief, T.A., El Mousa, S.E.D. and Tamamy, M.M.A.: 2004, Geoelectrical Survey to Delineate the Extension of the Water Bearing Formations in Wadi Gharandal, Southwest Sainai, Egypt. *Geophysical Society Journal,* 2(1): 75-84.

Zohdy, A.A.R.: 1975, Automatic interpretation of Schlumberger sounding curves using modified Dar Zarrouk functions. *Bulletin* 13 B-E, *U.S. Geological Survey*.

Zohdy, A.A.R.: 1989, A new method for the automatic interpretation of Schlumberger and Wenner sounding curve. *Geophysics,* 54(2): 245-253.

استكشاف المياه الجوفية في رفح ـ شبه جزيرة سيناء ـ مصر

محمود إسماعيل محمدين

المعهد القومي لعلوم البحار والمصايد – الإسكندرية - جمهورية مصر العربية

تم قياس 79 جسة كهربية (السبر العمودي) من خلال عدد 14 برفيل تم قياسها في منطقة رفح في شمال شرق سيناء لتحديد خزان المياه الجوفية في روسبيات زمن الرباعي. نتيجة تحليل هذه النتائج تم عمل برفيلات كهربية لتوضيح الجيولوجيا السطحية وتحت السطحية. اعتمادا علي الأعماق والمقاومات الكهربية تم تحديد خزان المياه الجوفية.

إن الطرق الجيوكهربية تعطي معلومات عن الجيولوجيا تحت السطحية والتراكيب الجيولوجية المؤثرة علي منطقة الدراسة. هذا بالإضافة إلي بعض المعلومات عن المكونات للصخور المختلفة لزمن الرباعي والتراكيب الجيولوجية التي قد تؤثر علي المياه الجوفية والتراكيب الجيولوجية بمنطقة رفح شمال سيناء.

تفسير النتائج الكهربية أظهرت أن المنطقة يتألف من ثلاث طبقات. الطبقة العليا تتكون من الحصى بالغ الارتفاع النسبي لقيم المقاومة الكهربائية ، والثانية تتكون طبقة من الرمل (طبقة المياه الجوفية) وهي متوسطة لقيم المقاومة الكهربائية(8-204 اوم – متر) ، والثالثة تتكون طبقة من الطين (حاجز للمياه) منخفضة نسبيا لقيم المقاومة الكهربائية.الطبقة الثانية طبقة واعدة للغاية للمياه الجوفية. ويبلغ الحد الأقصى لعمق المياه يتراوح ما بين 3.6 إلى 181 متر.

التراكيب الجيولوجية التي تؤثر على المنطقة في إطار تحليل النتائج الكهربية توضح أن هذه المنطقة معرضة لمجموعة من الفوالق المنطقة الوسطي للفوالق هي التي تحتوي علي المياه الجوفية. سمك هذه الطبقة يزداد في اتجاه الجنوب. الإزاحة السفلية لمجموعة الفوالق الشمالية في اتجاه الجنوب والإزاحة السفلية لمجموعة الفوالق الجنوبية في اتجاه الشمال . هذه الفوالق تشكل ما يسمي الفولق الحوضية أو الأخدود أو الجربن.